AAS 24-313

DYNAMICS LEVERAGED IN LONG-TERM STATIONKEEPING STRATEGIES FOR MULTI-BODY ORBITS

Dale A. P. Williams[*], Kathleen C. Howell[†], and Diane C. Davis[‡]

Increased interest in the development of cislunar space requires greater intuition for the operation of spacecraft in multi-body orbits. Many such orbits are linearly unstable, and an orbit maintenance strategy is required to secure a spacecraft near some desired reference motion. The development of effective stationkeeping approaches is facilitated by improved understanding of the variational dynamics near a periodic orbit. In this investigation, Floquet Theory is applied to explore the underlying dynamics leveraged and controlled by several different orbit maintenance approaches. The dynamical requirements for long-term stationkeeping effectiveness are also examined.

INTRODUCTION

Recent years have seen renewed international interest in extending the reach of spaceflight missions beyond Earth orbit and into the cislunar region or beyond. The upcoming Artemis series of missions planned by NASA, along with international partners, aims to return humans to the lunar surface for the first time since 1972.[1] Components of the Artemis missions are planned to fly in multi-body orbits that leverage the gravitational influence of both the Earth and the Moon.[2] Moreover, the National Cislunar Science and Technology Strategy highlights objectives for economic and scientific growth, cooperation with international partners, and infrastructure capabilities as priorities for the United States in the cislunar region.[3] Development and understanding of operational strategies for this region are, therefore, of great importance.

Dynamics within the cislunar region are complex, varied, and often modeled within the context of the Circular Restricted Three Body Problem (CR3BP). Within this multi-body dynamical model, periodic orbits are known to exist and often serve as a starting point for mission design applications.[2,4] Many periodic orbits in the CR3BP are linearly unstable and small variations from the reference orbit eventually result in spacecraft departure. As a result, orbit maintenance strategies must be developed to secure a spacecraft near some desirable baseline motion in the presence of inevitable operational errors.

Numerous investigations of the orbit maintenance problem for multi-body orbits are available, and many updated stationkeeping approaches are in various stages of development. Crossing control strategies remain a successful option after being employed for several Sun-Earth libration point missions, as well as for the ARTEMIS/THEMIS and CAPSTONE missions in the Earth-Moon system.[4–7] A modified crossing control approach is planned for the Gateway orbital outpost, a key component of the upcoming Artemis missions.[8] Target Point Approaches (TPA), originally

[*]Graduate Student, School of Aeronautics and Astronautics, Purdue University, West Lafayette, IN 47907; will1738@purdue.edu

[†]Hsu Lo Distinguished Professor, School of Aeronautics and Astronautics, Purdue University, West Lafayette, IN, 47907; howell@purdue.edu

[‡]Aerospace Engineer, NASA Johnson Space Center, Houston, TX, 77058; diane.c.davis@nasa.gov

developed by Howell and Keeter,[9] also serve as notable background efforts. One potential TPA was leveraged in stationkeeping operations for the Genesis mission launched in 2001.[10] Other authors explore the information available from the Cauchy-Green Strain Tensor[11–13] (CGT) or from Floquet Theory[13–16] to accomplish the orbit maintenance objective. All of these strategies may be more or less appropriate depending on mission requirements.

While significant effort is often devoted to the development of effective stationkeeping techniques, it is equally important to investigate the underlying dynamics that these approaches leverage. The dynamical significance of maneuver directions associated with orbit maintenance approaches are discussed by numerous authors such as Murlidharan and Howell,[12] Folta et al.,[7] and Davis et al.[8] Farrés et al. leverage information available from Floquet Theory to highlight similarities between crossing control and Floquet Mode Control (FMC) strategies when the FMC problem is solved to minimize the magnitude of a stationkeeping maneuver.[17] Williams et al. also apply Floquet Theory to investigate the effects of stationkeeping maneuvers on post-maneuver distributions of spacecraft variational state components associated with different characteristic behaviors.[13] This investigation extends the work of Farrés et al. and Williams et al. to clearly highlight dynamical requirements for successful long-term orbit maintenance approaches.

DYNAMICAL SYSTEMS THEORY

Throughout this investigation, the CR3BP is employed as the dynamical model for spacecraft motion. The CR3BP equations of motion are constructed in a rotating frame and are well documented by previous authors.[13] One integral of motion, the Jacobi Constant, is known to exist, and the model possesses a Hamiltonian structure.[18,19] Let $\boldsymbol{x}(t) = [\boldsymbol{r}(t) \quad \boldsymbol{v}(t)]^T$ represent the six-dimensional position and velocity state of a spacecraft in the CR3BP rotating frame, where boldface symbols imply vector quantities. Of particular interest for the stationkeeping problem is a spacecraft variational state measured with respect to some known trajectory, $\boldsymbol{x}^*(t)$. The first-order evolution of a variational state defined by $\delta\boldsymbol{x}(t) = \boldsymbol{x}(t) - \boldsymbol{x}^*(t)$ is described by state transition matrix (STM) such that

$$\delta\boldsymbol{x}(t) = \Phi(t, t_0)\delta\boldsymbol{x}(t_0). \tag{1}$$

Due the linear form of the STM, variational dynamics are often more amenable for analysis as compared to the full nonlinear space.

Floquet Theory

When a reference is periodic (i.e., $\boldsymbol{x}^*(t) = \boldsymbol{x}^*(t+\tau)$, where τ is the orbital period), the state transition matrix is simplified via the application of Floquet theory. Specifically, the state transition matrix is decomposed as

$$\Phi(t, t_0) = F(t)e^{\mathcal{J}(t-t_0)}F^{-1}(t_0), \tag{2}$$

where $F(t) = F(t+\tau) = [\boldsymbol{f}_1(t) \quad \cdots \quad \boldsymbol{f}_6(t)]$ is a τ-periodic matrix containing the modal vectors, $\boldsymbol{f}_i(t)$, as columns, and $e^{\mathcal{J}(t-t_0)}$ is a block-diagonal exponential matrix defined by the characteristic exponents, η_i, associated with the periodic orbit.[13,14,17] This decomposition can always be constructed such that $F(t)$ and $e^{\mathcal{J}(t-t_0)}$ are real valued for all time, but the precise form of $e^{\mathcal{J}(t-t_0)}$ depends on the nature of the characteristic exponents (i.e., real, complex, purely imaginary, etc.).[19] The characteristic exponents are related to the eigenvalues of the monodromy matrix, λ_i, by

$$\eta_i = \frac{1}{\tau}\ln(\lambda_i). \tag{3}$$

Due to the symplectic structure of any CR3BP state transition matrix, these characteristic exponents must occur in positive and negative pairs.[13,18–20] Periodic orbits in this investigation possess a set of characteristic exponents such that

$$e^{\mathcal{J}(t-t_0)} = \begin{bmatrix} e^{\eta_1(t-t_0)} & 0 & 0 & 0 & 0 & 0 \\ 0 & e^{-\eta_1(t-t_0)} & 0 & 0 & 0 & 0 \\ 0 & 0 & \cos(\zeta(t-t_0)) & \sin(\zeta(t-t_0)) & 0 & 0 \\ 0 & 0 & -\sin(\zeta(t-t_0)) & \cos(\zeta(t-t_0)) & 0 & 0 \\ 0 & 0 & 0 & 0 & 1 & (t-t_0) \\ 0 & 0 & 0 & 0 & 0 & 1 \end{bmatrix}. \quad (4)$$

Here, η_1 is a positive, real number that defines the largest characteristic exponent of the periodic orbit and, due to the positive-negative pairing of characteristic exponents, $\eta_2 = -\eta_1$. Cosine and sine terms arise as a consequence of two purely imaginary characteristic exponents, η_3 and $\eta_4 = -\eta_3$, where $\Im(\eta_3) > 0$. The associated frequency, ζ, is defined by $\zeta = \Im(\eta_3)$.[13,14,21] A pair of unity entries on the diagonal are associated with two characteristic exponents that are equal to zero and occur as a consequence of the autonomous and Hamiltonian structure of the CR3BP equations of motion.[19] These characteristic exponents are commonly denoted the "trivial pair," because they are present for *any* CR3BP periodic orbit. Note that similar matrices can be constructed for orbits with different stability characteristics.

The Floquet decomposition in Equation (2) provides a useful change of coordinates for analyzing the evolution of variations in the vicinity of a periodic reference. Define the modal coordinate vector, $\boldsymbol{\alpha}(t)$, such that

$$\delta\boldsymbol{x}(t) = F(t)\boldsymbol{\alpha}(t). \quad (5)$$

From Equations (1) and (2), it is clear that

$$\boldsymbol{\alpha}(t) = e^{\mathcal{J}(t-t_0)}\boldsymbol{\alpha}(t_0). \quad (6)$$

Thus, for periodic orbits considered in this investigation, the components of the modal coordinate vector (termed the modal coordinates) exhibit different characteristic behavior associated with exponential growth (α_1), exponential decay (α_2), oscillation ($\alpha_{3,4}$), linear change (α_5), and a constant value (α_6). Furthermore, the growth of the unstable state component, α_1, is characterized by the time constant of the orbit, $t_c = 1/\eta_1$.[19,22] This quantity defines the time required for α_1 to grow by a factor of e. Note that, for orbits with different stability characteristics, the time-evolution of each of the modal coordinates will depend on the associated (modified) form of $e^{\mathcal{J}(t-t_0)}$. Advantages of the modal coordinate representation over the standard CR3BP Cartesian coordinates for describing variational state evolution near a periodic orbit are highlighted in Figures 1 and 2. Note from Figure 1 that the time history for each of the cartesian (position and velocity) state components is unpredictable, whereas each of the modal components plotted in Figure 2 display specific types of characteristic behavior.

Physically, the Floquet modes, $\boldsymbol{f}_i(t)$, associated with each of the modal components define the linear invariant subspaces of the periodic orbit. Specifically, $\boldsymbol{f}_1(t)$ defines the unstable direction at time t, whereas $\boldsymbol{f}_2(t)$ characterizes the stable direction. The complex-center subspace, spanned by $\boldsymbol{f}_3(t)$ and $\boldsymbol{f}_4(t)$, is associated with bounded, quasi-periodic motion near the reference orbit, in the linear sense. Two modal vectors, $\boldsymbol{f}_5(t)$ and $\boldsymbol{f}_6(t)$, are associated with the "trivial pair" of characteristic exponents and identify variations that define other nearby periodic solutions.[19,21]

Specifically, $\boldsymbol{f}_5(t)$ is directed along the phase-velocity direction and is consequently termed the "along orbit" direction, whereas $\boldsymbol{f}_6(t)$ defines a variation along the family of periodic orbits, of which the reference orbit is a member. Only variations with a nonzero component associated with the "along family" direction, $\boldsymbol{f}_6(t)$, produce a change in the integral of motion (i.e., Jacobi Constant or Hamiltonian).[21] Note from Figure 2(d) and Equation (6) that a nonzero value for α_6, associated with this "along family" direction, generates a linear change in α_5, associated with the "along orbit" direction. Physically, this linear change occurs as a result of the variation in the orbit period across a family of periodic orbits and represents a drift in phase with respect to the reference orbit.[19,21]

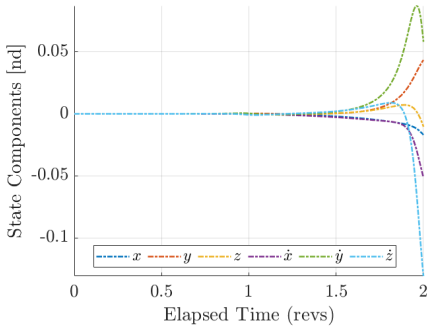

Figure 1: Example Variational State Evolution - Rotating Frame Coordinates

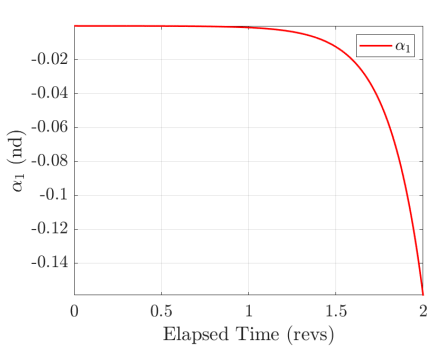

(a) Unstable Component (α_1)

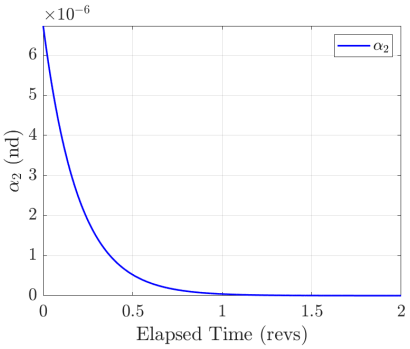

(b) Stable Component (α_2)

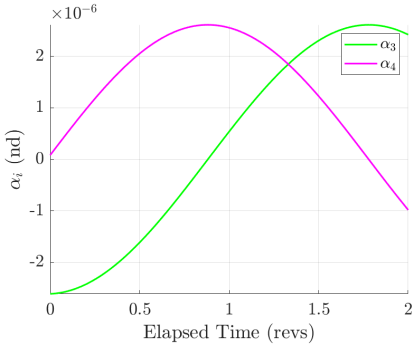

(c) Oscillatory Components ($\alpha_{3,4}$)

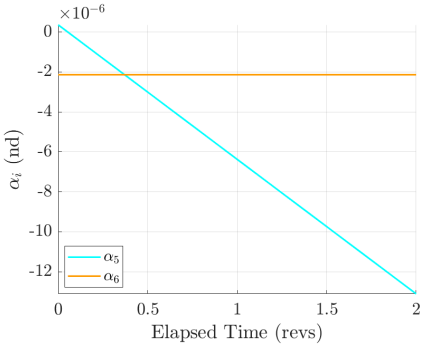

(d) Trivial Center Components ($\alpha_{5,6}$)

Figure 2: Example Variational State Evolution - Modal Coordinates

Periodic orbits in the CR3BP are not typically expressed analytically, and correspondingly, a numerical strategy is required to determine both $F(t)$ and the characteristic exponents of the orbit. Such a numerical approach leverages the monodromy matrix of the periodic orbit, $\Phi(t_0+\tau, t_0)$. Note from Equation (2) that

$$\Phi(t_0+\tau, t_0) = F(t_0)e^{J\tau}F^{-1}(t_0),$$

and $e^{\mathcal{J}\tau}$ is a matrix in real Jordan form. Hence, $F(t_0)$ is constructed from the generalized eigenvectors of the monodromy matrix. The monodromy matrix for any CR3BP periodic orbit is defective (possessing a unity eigenvalue with algebraic multiplicity equal to two and geometric multiplicity equal to one) and, therefore, careful steps are required to appropriately construct $F(t_0)$, as outlined in detail by Williams.[19] Once $F(t_0)$ is determined, along with the characteristic exponents, the matrix $F(t)$ is constructed for any time, t, from

$$F(t) = \Phi(t, t_0)F(t_0)e^{-\mathcal{J}(t-t_0)} \tag{7}$$

Recall that $F(t) = F(t+\tau)$, so it is only necessary to consider $t \in [t_0,\ t_0+\tau)$ to define the matrix for all time values.

Stretching and Restoring Subspaces

While the application of Floquet Theory inherently requires a periodic reference trajectory, the Singular Value Decomposition (SVD) is applied to extract useful information from any arbitrary STM associated with a fixed horizon time. The SVD decomposes the State Transition Matrix in terms of three matrices such that

$$\Phi(t, t_0) = U\Sigma\Xi^T. \tag{8}$$

Both U and Ξ are orthogonal matrices with columns $\boldsymbol{u}_i$ and $\boldsymbol{\xi}_i$, respectively, defining the left and right (orthonormal) singular vectors of the STM. The diagonal matrix, Σ, contains the associated singular values, ς_i. An equivalent expression for Equation (8) is, therefore,

$$\Phi(t, t_0)\boldsymbol{\xi}_i = \varsigma_i \boldsymbol{u}_i \qquad\qquad i = 1, 2, ...6.$$

It is clear that, if $\varsigma_i > 1$, an initial variation along $\boldsymbol{\xi}_i$ grows in magnitude over $[t_0,\ t]$, whereas if $0 < \varsigma < 1$, the magnitude of the six-dimensional variation decreases. Correspondingly, stretching and restoring subspaces are defined

$$S^+ = \text{span}\{\boldsymbol{\xi}_i\} \text{ s.t. } \varsigma_i > 1 \tag{9}$$

$$S^- = \text{span}\{\boldsymbol{\xi}_i\} \text{ s.t. } 0 < \varsigma_i < 1. \tag{10}$$

Any initial variation $\delta\boldsymbol{x}(t_0) \in S^+$ will grow in magnitude over the specified time horizon whereas any $\delta\boldsymbol{x}(t_0) \in S^-$ will decrease in magnitude.

Instead of considering the stretching and restoring subspaces associated with the full six-dimensional state vector, it may be advantageous to consider subspaces of the variational space associated with a characteristic change in *position* magnitude over a specified time horizon. To construct these subspaces, the state transition matrix is divided into submatrices such that

$$\Phi(t, t_0) = \begin{bmatrix} \Phi_{\boldsymbol{rr}} & \Phi_{\boldsymbol{rv}} \\ \Phi_{\boldsymbol{vr}} & \Phi_{\boldsymbol{vr}} \end{bmatrix},$$

and the 3×6 matrix, $\Phi_{\boldsymbol{r},\boldsymbol{rv}} = \begin{bmatrix}\Phi_{\boldsymbol{rr}} & \Phi_{\boldsymbol{rv}}\end{bmatrix}$, is defined. With respect to the reference trajectory, $\Phi_{\boldsymbol{r},\boldsymbol{rv}}$ relates an initial variation in the six-dimensional phase space to a downstream position error. The singular value decomposition of this matrix is

$$\Phi_{\boldsymbol{r},\boldsymbol{rv}} = \underline{U}\underline{\Sigma}\underline{\Xi}^T, \tag{11}$$

where

$$\underline{U} = \begin{bmatrix}\underline{\boldsymbol{u}}_1 & \underline{\boldsymbol{u}}_2 & \underline{\boldsymbol{u}}_3\end{bmatrix} \qquad \underline{\Xi} = \begin{bmatrix}\underline{\boldsymbol{\xi}}_1 & \underline{\boldsymbol{\xi}}_2 & \underline{\boldsymbol{\xi}}_3 & \underline{\boldsymbol{\xi}}_4 & \underline{\boldsymbol{\xi}}_5 & \underline{\boldsymbol{\xi}}_6\end{bmatrix},$$

$$\underline{\Sigma} = \begin{bmatrix}\underline{\varsigma}_1 & 0 & 0 & 0 & 0 & 0 \\ 0 & \underline{\varsigma}_2 & 0 & 0 & 0 & 0 \\ 0 & 0 & \underline{\varsigma}_3 & 0 & 0 & 0\end{bmatrix},$$

and $\underline{\varsigma}_1 \geq \underline{\varsigma}_2 \geq \underline{\varsigma}_3$. It is clear that $\underline{\boldsymbol{\xi}}_4$, $\underline{\boldsymbol{\xi}}_5$, and $\underline{\boldsymbol{\xi}}_6$ are mapped to the zero vector by $\Phi_{\boldsymbol{r},\boldsymbol{rv}}$ and define a basis for the variational subspace that reduces the variational position magnitude downstream to zero (under the linearized flow). Expressing $\underline{\boldsymbol{\xi}}_i$ in terms of its position and velocity components, i.e., $\underline{\boldsymbol{\xi}}_i = [\underline{\boldsymbol{\xi}}_i^{\boldsymbol{r}} \quad \underline{\boldsymbol{\xi}}_i^{\boldsymbol{v}}]^T$, select $\delta\boldsymbol{x}(t_0) = \underline{\boldsymbol{\xi}}_i / \|\underline{\boldsymbol{\xi}}_i^{\boldsymbol{r}}\|$ and, consequently, $\|\delta\boldsymbol{r}(t_0)\| = 1$. From Equation (11),

$$\Phi_{\boldsymbol{r},\boldsymbol{rv}}(t, t_0)\delta\boldsymbol{x}(t_0) = \frac{\underline{\varsigma}_i}{\|\underline{\boldsymbol{\xi}}_i^{\boldsymbol{r}}\|}\underline{\boldsymbol{u}}_i,$$

and $\|\delta\boldsymbol{r}(t)\| = \underline{\varsigma}_i \|\underline{\boldsymbol{u}}_i\| / \|\underline{\boldsymbol{\xi}}_i^{\boldsymbol{r}}\|$. As such

$$\frac{\|\delta\boldsymbol{r}(t)\|}{\|\delta\boldsymbol{r}(t_0)\|} = \underline{\varsigma}_i \frac{\|\underline{\boldsymbol{u}}_i\|}{\|\underline{\boldsymbol{\xi}}_i^{\boldsymbol{r}}\|}. \tag{12}$$

Hence, if $\underline{\varsigma}_i \|\underline{\boldsymbol{u}}_i\| / \|\underline{\boldsymbol{\xi}}_i^{\boldsymbol{r}}\| > 1$, the magnitude of the position variation associated with $\underline{\boldsymbol{\xi}}_i$ grows over the given time interval. Correspondingly, position-stretching and position-restoring subspaces are defined

$$\underline{S}^+ = \text{span}\{\underline{\boldsymbol{\xi}}_i\},\ \frac{\underline{\varsigma}_i \|\underline{\boldsymbol{u}}_i\|}{\|\underline{\boldsymbol{\xi}}_i^{\boldsymbol{r}}\|} > 1 \tag{13}$$

$$\underline{S}^- = \text{span}\{\underline{\boldsymbol{\xi}}_i\} \cup \text{span}\{\underline{\boldsymbol{\xi}}_4, \underline{\boldsymbol{\xi}}_5, \underline{\boldsymbol{\xi}}_6\},\ 0 \leq \frac{\underline{\varsigma}_i \|\underline{\boldsymbol{u}}_i\|}{\|\underline{\boldsymbol{\xi}}_i^{\boldsymbol{r}}\|} < 1. \tag{14}$$

The position-restoring subspace has practical use for orbit maintenance operations.

ORBIT MAINTENANCE STRATEGIES

As noted in the introductory section, a plethora of orbit maintenance strategies for multi-body orbits are available. Within this investigation, attention is restricted to two broad classes of stationkeeping methods: Floquet Mode Control (FMC) and Principal Stretching Direction Control (PSDC). Both FMC and PSDC schemes leverage information from the linearized variational dynamics to construct a maneuver that secures a spacecraft near some desired reference orbit within the full nonlinear model, under the presence of simulated operational errors. Throughout this investigation, the maneuver ($\Delta\boldsymbol{V}$) constructed in the linearized model is implemented "as-is" (i.e., without subsequent targeting) in the full nonlinear system.

Floquet Mode Control Strategies

Floquet Mode Control strategies explicitly enact control over the modal coordinate vector components (α_i) that define a spacecraft variational state. Traditionally, such strategies are formulated to eliminate the unstable component of the variational state, α_1, that is associated with exponential growth,[14,17] however, it is possible to enact control over other modes as well.[13,19] In the most general form,[13,19] FMC strategies are formulated to solve

$$\delta \boldsymbol{x}(t) = \mathcal{F}\boldsymbol{\alpha}_{aug}, \tag{15}$$

where

$$\mathcal{F} = \begin{bmatrix} F(t) & 0_{3\times 3} \\ & -I_{3\times 3} \end{bmatrix} \qquad\qquad \boldsymbol{\alpha}_{aug} = \begin{bmatrix} \boldsymbol{\alpha} \\ \Delta \boldsymbol{V} \end{bmatrix},$$

to minimize an objective function, J_{fmc}, defined in terms of a user-specified weighting matrix, W_{fmc}, and target vector, $\boldsymbol{b}_{fmc}$, as

$$J_{fmc} = \frac{1}{2}\|W_{fmc}\boldsymbol{\alpha}_{aug} - \boldsymbol{b}_{fmc}\|^2. \tag{16}$$

Through an appropriate choice of W_{fmc} and $\boldsymbol{b}_{fmc}$, effective control can be enacted over any mode of a periodic orbit and weighted against the maneuver magnitude, ΔV.

In this investigation, two Floquet Mode Control approaches are assessed. The first, termed Standard Floquet Mode Control, seeks to eliminate *only* the unstable component of a spacecraft variational state and minimizes the corresponding ΔV. This strategy is implemented by selecting $W_{fmc} = \text{diag}([10000 \quad 0 \quad \cdots \quad 0 \quad 1 \quad 1 \quad 1])$ and $\boldsymbol{b}_{fmc} = \boldsymbol{0}$. The second Floquet Mode Control Strategy, denoted Energy + State Floquet Mode Control, seeks to eliminate both the unstable and "along family" components of the variational state and weights the maneuver component magnitudes equally to the complex-center and "along orbit" state components. Energy + State Floquet Mode Control is a reasonable description of this strategy because eliminating the "along family" component of the spacecraft variational state corresponds to preventing a variation in the energy-like Jacobi Constant (or Hamiltonian) from the reference orbit.[19,21] Note, however, that neither the Jacobi Constant nor Hamiltonian represent the total energy in the system; both are merely "energy-like" integrals for the system motion. In the Energy + State FMC scheme, W_{fmc} and $\boldsymbol{b}_{fmc}$ are selected such that $W_{fmc} = \text{diag}([10000 \quad 0 \quad 1 \quad \ldots \quad 1 \quad 10000 \quad 1 \quad 1 \quad 1]$ and $\boldsymbol{b}_{fmc} = \boldsymbol{0}$. For both FMC approaches, the required variational state, $\delta\boldsymbol{x}(t)$, and modal matrix, $F(t)$, are constructed from an isochronous correspondence with the reference orbit.

Principal Stretching Direction Control Strategies

Principal Stretching Direction Control (PSDC) strategies construct an impulsive maneuver that places a spacecraft into the restoring, or position restoring, subspace associated with the reference trajectory and a specified horizon time. When the full-state restoring subspace (S^-) is the focus, the strategy is denoted as State PSDC. Converesely, if the position-restoring subspace is employed ($\underline{S}^-$), the strategy is termed a Position PSDC, or PPSDC, approach. Recall that a horizon time is required to generate either S^- or $\underline{S}^-$. In this investigation, the horizon time associated with the i^{th} orbit maintenance maneuver (OMM) is selected to be $[t_i,\, t_{i+1}]$, where t_i represents the epoch of the current maneuver and t_{i+1} the epoch of the next allowable OMM. This specific representation

of horizon time is illustrated in Figure 3 and ensures that the *post-manevuer* variational state (or position) magnitude decreases by the epoch of the next permitted OMM.

Mathematically, PSDC strategies are implemented similarly to Floquet Mode Control.[19] For a State PSDC scheme, a maneuver is constructed via the solution of the linear system of equations

$$\delta \boldsymbol{x}(t_i) = \begin{bmatrix} \Xi & 0_{3\times 3} \\ & -I_{3\times 3} \end{bmatrix} \begin{bmatrix} \boldsymbol{\beta} \\ \Delta \boldsymbol{V} \end{bmatrix} = \mathcal{G}\boldsymbol{\beta}_{aug}, \tag{17}$$

that minimizes the objective function

$$J_{PSDC} = \frac{1}{2}\|W_{PSDC}\boldsymbol{\beta}_{aug}\|^2. \tag{18}$$

When a PPSDC approach is desired, Ξ is replaced with $\underline{\Xi}$ in Equation (17). The diagonal weighting matrix, W_{PSDC}, is defined to place large weights on the components of $\boldsymbol{\beta}$ that are associated with the stretching subspace, thereby ensuring a solution that functionally eliminates this undesirable behavior. Throughout this investigation, numerical weights for undesirable state components are selected to be 10,000, whereas weights for permitted state components associated with the restoring, or position restoring, subspace are equal to zero. Components of the constructed maneuver, $\Delta \boldsymbol{V}$, are weighted with a numerical value equal to unity.

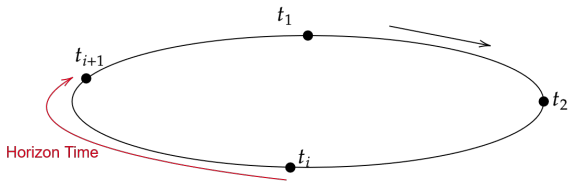

Figure 3: PSDC Horizons

Two Position PSDC approaches, as well as the standard State PSDC method,[13] are evaluated in this investigation. In the first Position PSDC strategy, termed Standard PPSDC, a maneuver that simply moves a spacecraft into the position restoring subspace, $\underline{S}^-$, is constructed. From the structure of the Singular Value Decomposition for $\Phi_{\boldsymbol{rr},\boldsymbol{rv}}$, it is possible to further restrict the post-maneuver variational state to exist with in a subspace of $\underline{S}^-$ defined by null($\Phi_{\boldsymbol{rr},\boldsymbol{rv}}$) that is predicted to reduce the position variation of a spacecraft to zero over the prescribed horizon time. This approach is denoted Genesis PPSDC, since a nearly identical strategy was implemented in operations for the GENESIS mission.[10]

ORBIT MAINTENANCE EXAMPLE - L_2 HALO ORBIT

While some successful stationkeeping approaches do not require a precise baseline orbit[6,7] an objective for many orbit maintenance strategies is to secure a spacecraft near some desired reference motion in the presence of unplanned variations from the nominal trajectory. Such a "strict" approach is advantageous in cases when mission requirements require close adherence to the planned reference motion. Performance of any orbit maintenance algorithm is inherently a function of these errors, resulting from imperfect maneuver execution, navigation, orbit injection, and system modeling, among other possible sources. In this investigation, orbit maintenance of an L_2 halo orbit in the

Earth-Moon system is assessed. The selected orbit is depicted in Figure 4, along with the arbitrarily assumed orbit injection location. Parameters for this particular orbit are provided in Table 1. A 500 revolution mission lifetime, corresponding to approximately twenty years, is selected to be representative of relatively long mission lifetimes expected for future cislunar missions.[8] Modeled errors are summarized in Table 2. Consideration of orbit injection and navigation errors is consistent with those employed by Gómez et al.[16] and maneuver execution error is simulated identically to Davis et al.[8] A minimum allowable maneuver magnitude is also incorporated for all implemented strategies. Specifically, orbit maintenance maneuvers with a maneuver magnitude less than 3 cm/s are waived, consistent with Davis et al.[8]

Table 1: Reference Halo Orbit Parameters

τ (days)	Jacobi Constant	Time Constant (days)	Time Constant (revs)
14.6368	3.1300	2.1854	0.1493

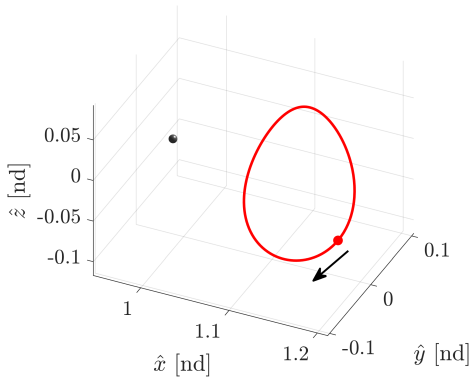

Figure 4: Reference Halo Orbit and Injection Location

Table 2: Error Modeling

Category	Error Type	1σ Value	Location
Navigation	Position	1 km	24 hours prior to maneuver
	Velocity	1 cm/s	
Orbit Injection	Position	1 km	Injection location on orbit
	Velocity	1 cm/s	
Maneuver Execution	Relative	0.5%	Each executed maneuver
	Fixed	0.0473 cm/s	
	Direction	$1/3^\circ$	

The performance of any orbit maintenance approach that is based on a reference trajectory is also a function of maneuver frequency and placement. Within this investigation, orbit maintenance maneuvers are permitted at epochs that correspond to arrivals at specific locations along the baseline orbit. These maneuver epochs are spaced by one quarter (1/4) revolution along the reference halo orbit, and the associated OMM locations are depicted in Figure 5. For all PSDC strategies, the horizon time for determining stretching and restoring subspaces is, therefore, 1/4 of the orbit period (or about 3.7 days). Note that the selected epoch spacing is between one and two orbit time constants. This selection for maneuver spacing bounds the maximum possible growth of α_1, the unstable variational state component, above by a factor of e^2 (approximately 7.4).

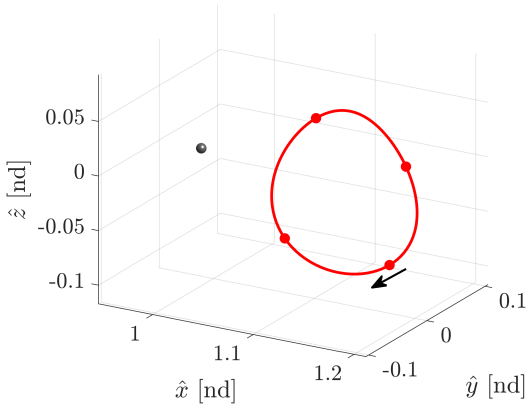

Figure 5: Maneuver Locations on Baseline L_2 Halo

For the five orbit maintenance strategies outlined previously, 500 Monte Carlo trials are conducted to estimate an annual orbit maintenance cost in terms of ΔV, as well as a total cost over the mission lifetime. The results appear in Table 3. Recall that orbit maintenance maneuvers are constructed based upon the linearized variational dynamics and are implemented "as-is" (i.e., without subsequent targeting) in the full nonlinear system. Strategies for which values are not reported indicate a failure of the approach to maintain a spacecraft within 20,000 km of the isochronous state on the reference orbit. From Table 3, it is clear that all successful orbit maintenance strategies posses a comparable mean annual stationkeeping cost. However, this result should not be generalized to other orbits, or even to different maneuver placement strategies within the specified orbit of interest. While orbit maintenance costs across successful strategies are comparable, the performance of each of these methods differs in terms of controlling position variation with respect to the reference orbit. Representative plots of isochronous position error for 15 Monte Carlo trials associated with each of the three successful strategies are provided in Figure 6. Note that, despite the comparable orbit maintenance costs, the Energy + State FMC strategy is associated with significantly higher position variation from the baseline orbit. This result is not necessarily surprising; recall that the PPSDC approaches explicitly seek to control position variations, whereas the Energy + State FMC method does not.

Table 3: Orbit Maintenance Cost by Strategy - 500 Monte Carlo Trials, 500 Revolution Mission

Strategy	Mean Total ΔV (m/s)	Std. Dev. Total (m/s)	Mean Annual ΔV (m/s)	Std. Dev. Annual (m/s)
Standard FMC	-	-	-	-
Energy + State FMC	241.0627	4.5532	12.0311	0.2272
Standard PPSDC	243.9701	4.5541	12.1762	0.2273
Genesis PPSDC	249.5727	4.2212	12.4558	0.2107
State PSDC	-	-	-	-

DYNAMICAL CHARACTERISTICS OF SUCCESSFUL STRATEGIES

Insight into the fundamental dynamical characteristics that the three successful orbit maintenance approaches leverage is available by viewing the variational state evolution in terms of modal coordinates. Representative plots of the modal coordinate evolution for a single Monte Carlo trial for each

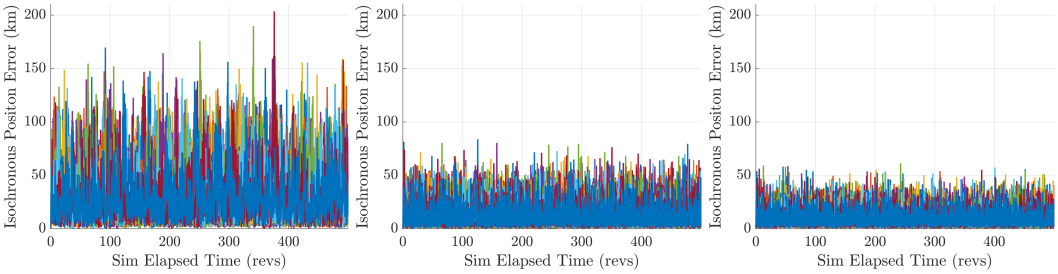

(a) Energy + State FMC (b) Standard PPSDC (c) Genesis PPSDC

Figure 6: Representative Position Errors for Successful Strategies

strategy appear in Figures 7-9. The top row in each of Figures 7-9 displays the modal coordinate evolution over the entire 500 revolution mission lifetime, whereas the bottom row depicts a 10 revolution subset that highlights the characteristic modal coordinate behavior more clearly. Dynamical similarities are observed across the three approaches.

Unstable Subspace

For each of the three successful orbit maintenance approaches considered, the component of a spacecraft variational state associated with the unstable subspace is well controlled. Recall that α_1 represents this component of the variational state and naturally grows at an exponential rate determined by the time constant of the periodic orbit. From Figure 7, it is clear that orbit maintenance maneuvers associated with each of the three effective strategies reset this modal coordinate to a value near zero, thus preventing unchecked exponential growth in the unstable subspace for the orbit. While the Energy + State FMC method is formulated to control the unstable state component explicitly, the same is not true for the two PPSDC approaches. The time-histories in Figure 7 suggest, unsurprisingly, that effective control over the unstable component of a spacecraft variational state is required for successful long-term orbit maintenance.

Stable Subspace

In contrast to the behavior associated with the unstable subspace, effective orbit maintenance strategies appear to *increase* the component of a spacecraft variational state associated with the stable subspace of the orbit. Recall that α_2, representing this state component, naturally exhibits exponential decay characterized by the time constant for the orbit. Correspondingly, orbit maintenance strategies that increase α_2 are not expected to be problematic. In fact, because the variational subspace of the orbit is spanned by $\boldsymbol{f}_{1-6}$, an orbit maintenance maneuver that decreases the magnitude of one component of the variational state (e.g., α_1), must generally increase the magnitude of some other component (e.g., α_2), since spacecraft position is unchanged by an impulsive OMM. It is advantageous that the increased component decays naturally over time.

Complex Center Subspace

Recall that the complex center subspace is associated with quasi-periodic motion in the vicinity of the reference orbit. Viewed in terms of modal coordinates, this quasi-periodic motion is observed

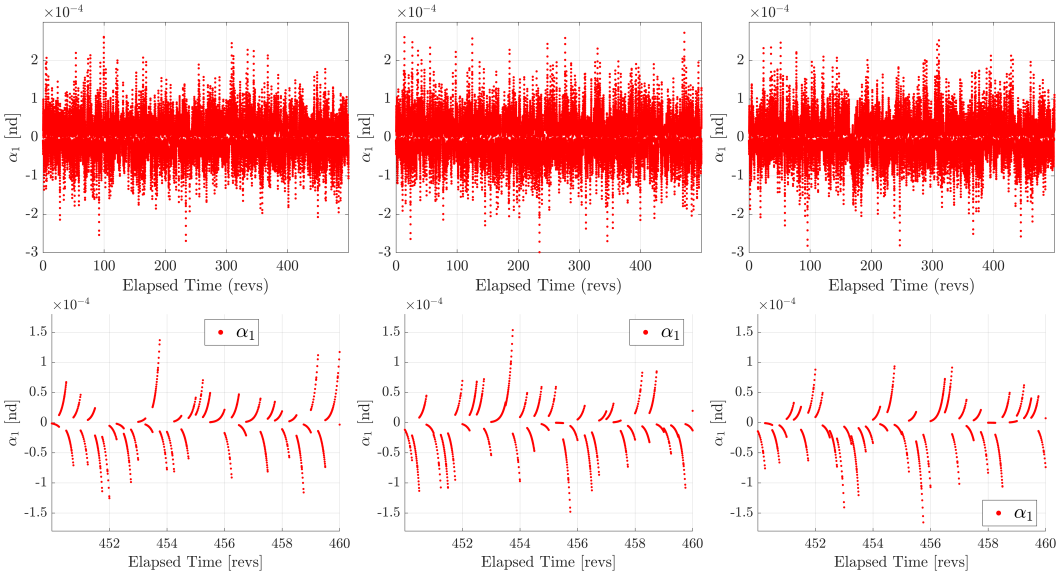

(a) Energy + State FMC (b) Standard PPSDC (c) Genesis PPSDC

Figure 7: Representative Behavior - Unstable Subspace

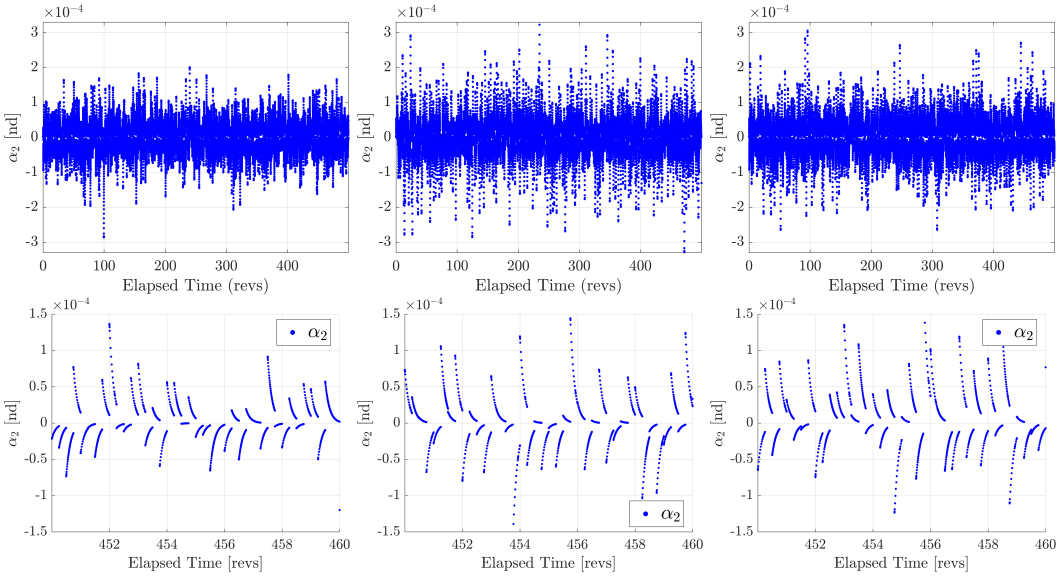

(a) Energy + State FMC (b) Standard PPSDC (c) Genesis PPSDC

Figure 8: Representative Behavior - Stable Subspace

as a sinusoidal evolution of α_3 and α_4, and depicted previously in Figure 2. From Figure 9, it is clear that the three successful orbit maintenance strategies disrupt this natural oscillatory behavior. This disruption is not, generally, expected to be required for successful orbit maintenance because the natural oscillatory behavior is predicted to be bounded. However, it is desirable to prevent orbit maintenance maneuvers from resulting in excessive growth of these state components; in such a case, the linearized approximation for variational motion may break down. It is notable that

the Energy + State FMC approach seems to result in generally larger values of α_3 and α_4 over the mission lifetime. This observation may explain, in part, why the Energy + State approach is associated with larger position errors as compared to the PPSDC methods.

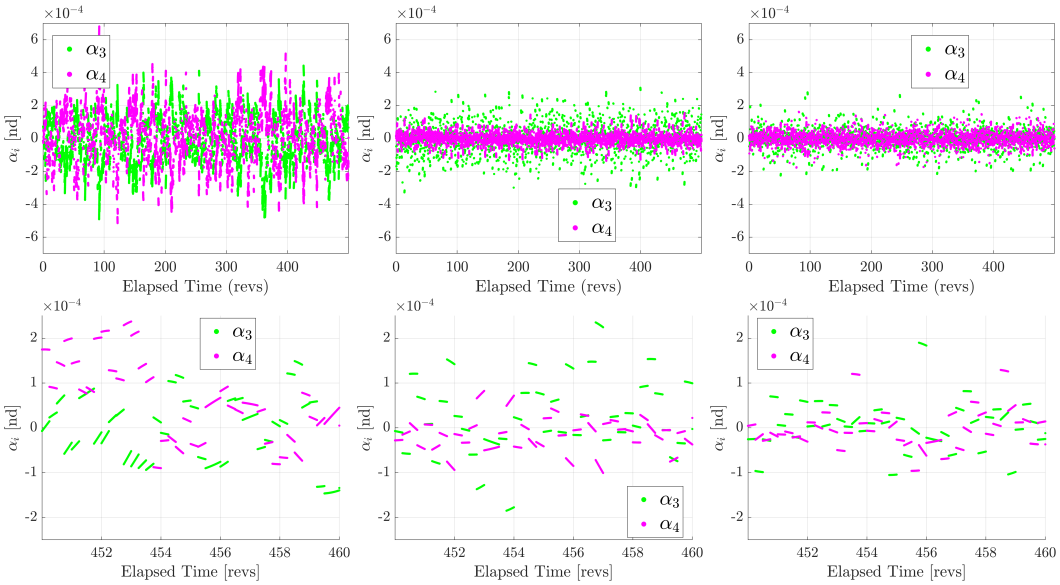

(a) Energy + State FMC (b) Standard PPSDC (c) Genesis PPSDC

Figure 9: Representative Behavior - Complex Center Subspace

Trivial Center Subspace

For all three successful orbit maintenance strategies, Figure 10 indicates that α_6, associated with the "along family" direction and a nonzero variation in the energy-like Jacobi Constant, is well-maintained to a value near zero. Recall that a nonzero value of α_6 is associated with a linear change in α_5, describing the "along orbit," or phasing, direction. The slope of this linear change is determined by the value of α_6, that remains constant under the linearized dynamics when no maneuver is applied. It is intuitive, then, that efficient orbit maintenance strategies maintain the "along family" component of a spacecraft variational state near zero to prevent such a drift in phase. Controlling this mode is analagous to maintaining any variation in the energy-like Jacobi Constant (or Hamiltonian) to a small value. Note that the Energy + State FMC approach seeks to accomplish this objective explicitly, whereas the two PPSDC strategies do not. Correspondingly, slightly greater values of α_6 are observed for the PPSDC approaches. All three successful strategies also prevent excessive growth in the magnitude of α_5, indicating that orbit phase is well maintained by these orbit maintenance methods.

DYNAMICAL CHARACTERISTICS OF UNSUCCESSFUL STRATEGIES: THE STANDARD FMC APPROACH

A modal coordinate representation of spacecraft variational state evolution can also be leveraged to elucidate modes of failure for ineffective orbit maintenance strategies. The results from these types of analysis are particularly illuminating in the case of the Standard FMC approach. Recall

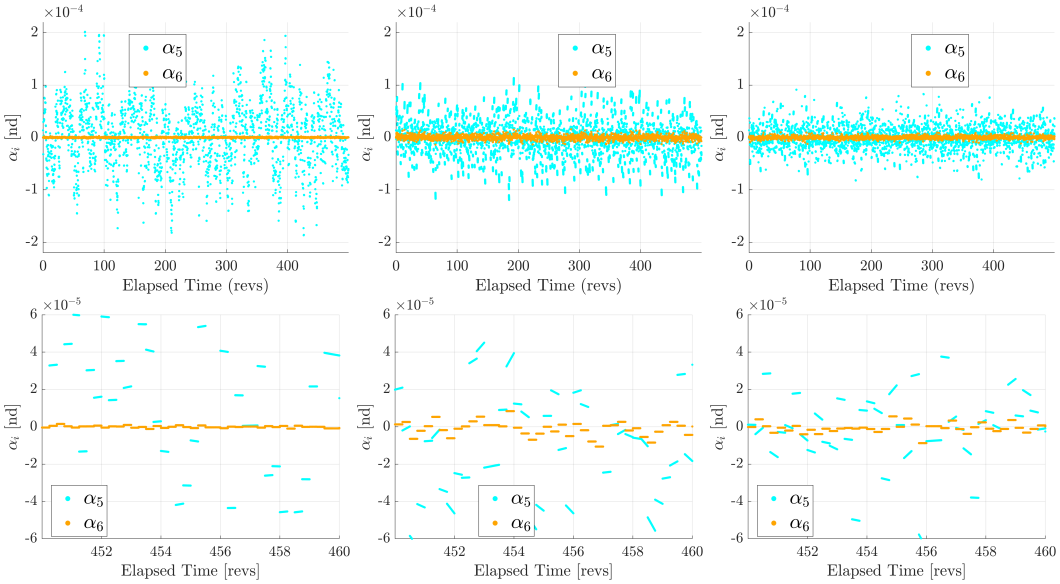

(a) Energy + State FMC (b) Standard PPSDC (c) Genesis PPSDC

Figure 10: Representative Behavior - Trivial Center Subspace

that this orbit maintenance strategy is formulated to eliminate *only* the unstable component of a spacecraft variational state and to minimize the corresponding maneuver magnitude. For a subset of 15 Monte Carlo trials, representative plots of the isochronous position error magnitude for the Standard FMC approach are plotted in Figure 11. For all trials, oscillatory behavior is observed in addition to increasing secular growth. Note that the time of divergence for this particular orbit maintenance algorithm varies widely, even within a small subset of 15 Monte Carlo Trials. While Standard FMC is not effective for the specified 20-year mission duration, it is possible that such this could be feasible in the short term, if some secular growth in variation from the reference orbit is permissible.

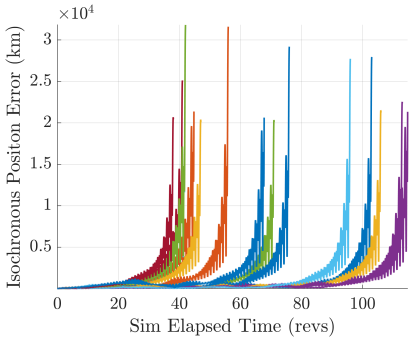

Figure 11: Representative Position Error Plots - Standard FMC

It is quickly observed that the mode of failure for the Standard FMC approach is *not* an inability to control the unstable component of a spacecraft variational state. Plots of the unstable and stable modal coordinate time histories are presented for twenty revolutions of a representative Monte Carlo trial associated with this scheme in Figure 12. Similar to the successful orbit maintenance

approaches, maneuvers constructed using the Standard FMC approach reset the unstable variational state component to a near-zero value. Recall that the Standard FMC strategy is, in fact, formulated to eliminate the unstable state component, so this behavior is expected. The effect of the Standard FMC scheme on α_2 is also similar to the successful orbit maintenance approaches. In both cases, executed orbit maintenance maneuvers increase the magnitude of the naturally-decaying stable component of the variational state.

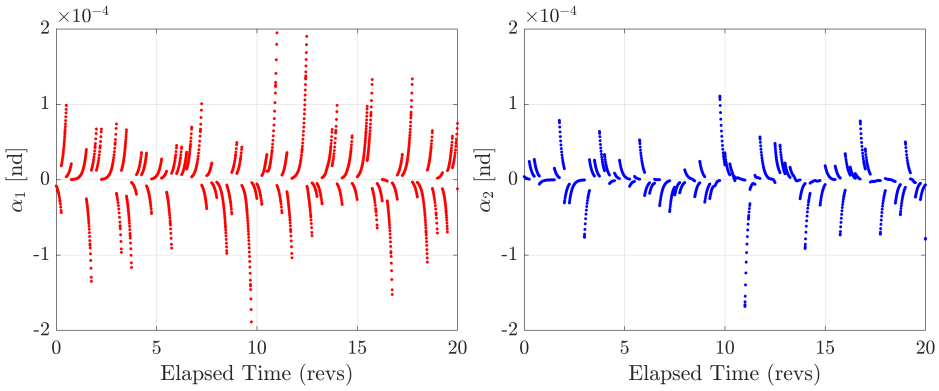

(a) Unstable Coordinate (b) Stable Coordinate

Figure 12: Hyperbolic Modal Coordinate Histories - Standard FMC

Failure of the Standard FMC scheme can, therefore, be attributed to insufficient control over the center modes of the reference orbit (defined by α_{3-6}). Representative time histories of these four modal coordinates are plotted for a single Monte Carlo trial in Figure 13. From Figure 13(a), it is apparent that the natural oscillatory behavior of the complex center state components is preserved under the Standard FMC approach. Recall that the Standard FMC approach seeks only to eliminate the *unstable* component of the variational state, so the persistence of this behavior is not unexpected. In fact, some growth in the complex center components is observable in Figure 13(a). The formulation of the Standard FMC enacts *no* control over α_{3-4}, so while this growth may not always be present, it is not actively prevented by the orbit maintenance algorithm. Over time, excessive growth in the complex center state components may result in sufficient drift from the reference motion that the linearized variational dynamics, necessary for any FMC strategy, are no longer valid, resulting in accelerated departure from the desired orbit.

More significant than the lack of control over the complex center components is the failure of the Standard FMC strategy to effectively control the trivial center components, α_{5-6}. From Figure 13(b), it is clear that large secular growth associated with α_5 is present, indicative of a drift in phase with respect to the reference periodic orbit. This drift in phase is partially associated with ineffective control over α_6. Recall that α_6 defines the component of a spacecraft variational state that is associated with the "along family" direction and a variation in the system integral of motion (Jacobi Constant or Hamiltonian) with respect to the baseline orbit. When the value of α_6 is nonzero, a linear change is also observed in α_5 as a consequence of the variation of the orbit period between periodic orbit family members. Hence, failure to maintain the value of α_6 close to zero will inherently produce a phase drift with respect to the isochronous baseline, introducing a mode of failure into the Standard FMC strategy.

More than simply failing to maintain a near zero-value of α_6, the Standard FMC approach actively

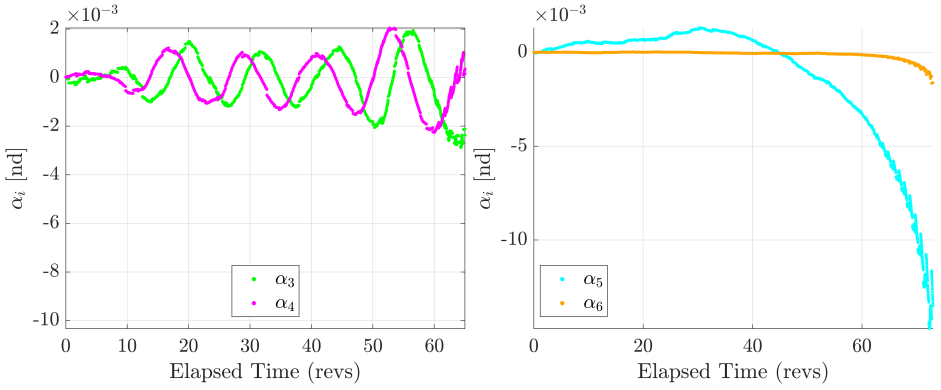

(a) Complex Center (b) Trivial Center

Figure 13: Center Modal Coordinate Histories - Standard FMC

introduces change in this state component. Under the natural linearized dynamics, α_6 remains a constant value. From Figure 14(a), it is clear that α_6 demonstrates appreciable growth in magnitude over time, indicating that successive OMMs produce a variation in Jacobi Constant with respect the baseline motion. These OMMs result in a "slide" along the associated family of periodic orbits, as depicted in Figures 14(b) and 14(c). This behavior is prevented in the successful Energy + State FMC approach by explicitly eliminating the "along family" component of the spacecraft variational state. For an orbit maintenance strategy to be effective, it therefore seems necessary to control both the unstable component of a spacecraft variational state, *and* the "along family" component.

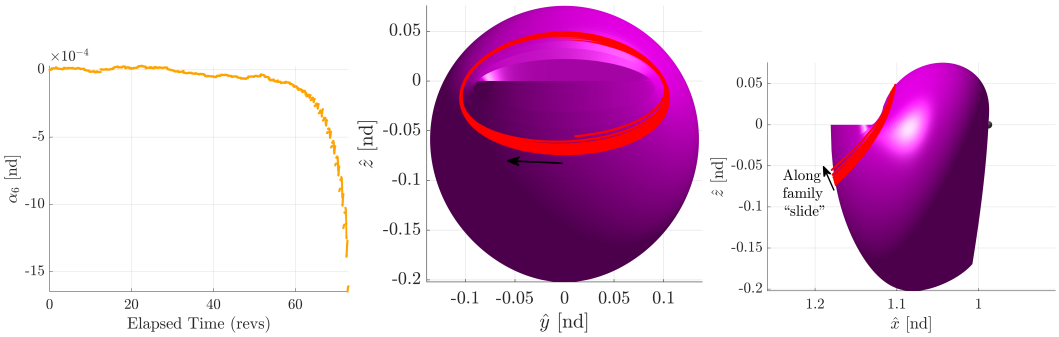

(a) "Along Family" Component (b) yz View (c) xz View

Figure 14: Along Family Drift and the Standard FMC Strategy

DYNAMICAL CHARACTERISTICS OF UNSUCCESSFUL STRATEGIES: THE STATE PSDC APPROACH

An investigation of the modal coordinate evolution associated with the State PSDC approach is also possible, but is less useful for identifying the mechanisms of failure associated with this strategy as compared to the Standard FMC scheme. Representative plots of the modal coordinate history for a single Monte Carlo trial of the State PSDC approach are displayed in Figure 15. From Figure 15, it appears as though this orbit maintenance algorithm generates maneuvers that actually *increase* some or all of the modal coordinate magnitudes, including α_1 (the unstable component).

Clearly, this behavior is undesirable and results in an extremely rapid departure from the reference orbit.

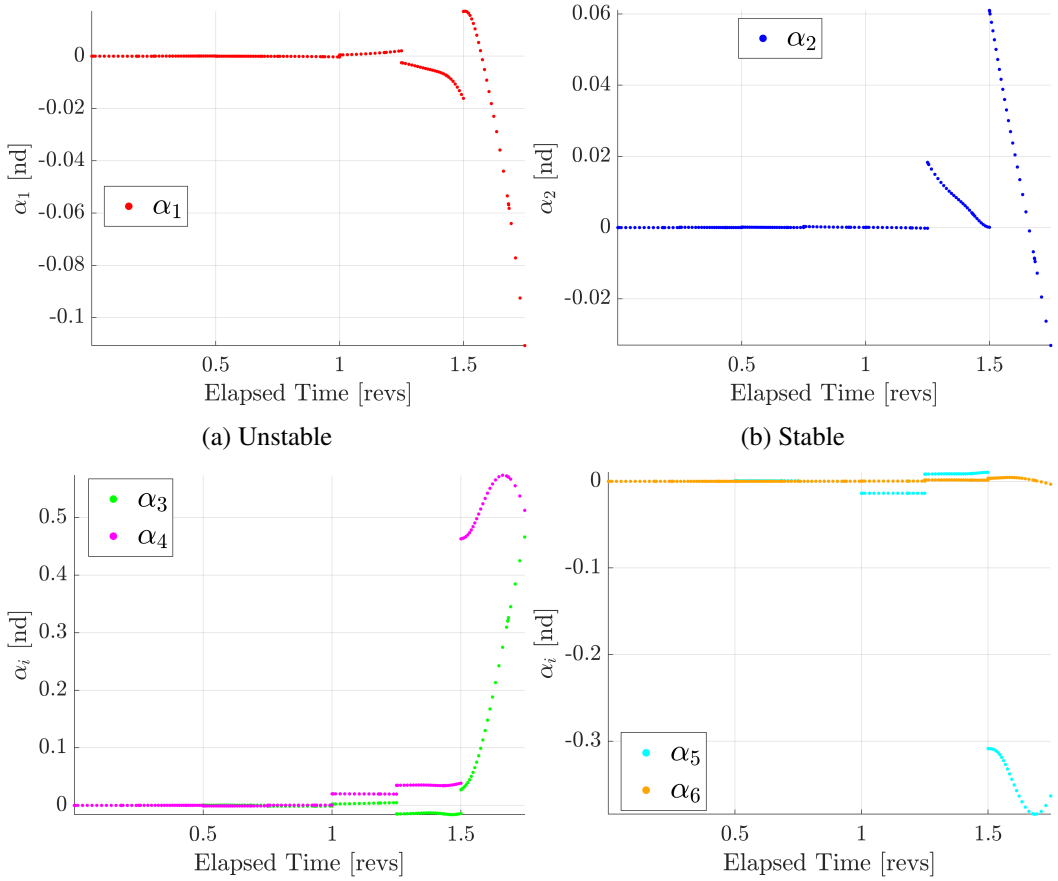

(a) Unstable (b) Stable

(c) Complex Center (d) Trivial Center

Figure 15: Representative State PSDC Modal Coordinate History

More insight into the failure of the State PSDC strategy is produced by exploring the evolution of the magnitude of $\delta\boldsymbol{x}(t)$ over time. A representative plot of this six-dimensional (isochronous) variational state error appears in Figure 16. A characteristic stair-step pattern is observed, where a vertical jump in the value of isochronous state error is associated with the application of an impulsive orbit maintenance maneuver. Note that between each of these discontinuities, a decrease in the mangitude of the state error is clear. Recall that the State PSDC scheme is formulated such that the *post-maneuver* variational state exists within the restoring subspace, S^-, associated with the selected horizon time. These decreases in variational state magnitude are, correspondinigly, characteristic of a post-maneuver state that exists within S^-. However, the applied maneuvers (associated with the vertical jumps in Figure 16) actually increase the magnitude of the variational state error *more* than the corresponding restoration and result in the failure of the State PSDC strategy. Note that the State PSDC approach can be effective in other orbits,[13] and it is possible that a change in the horizon time selection or maneuver placement could produce successful results for the halo orbit in this investigation. However, the results of this investigation highlight that State PSDC is not always an effective orbit maintenance approach.

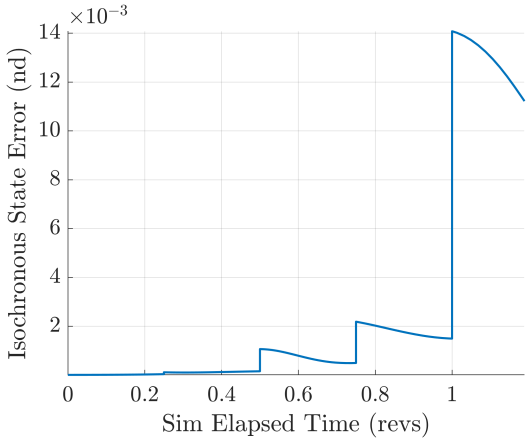

Figure 16: Representative Isochronous State Error vs. Time (State PSDC)

CONCLUDING REMARKS

In this investigation, the utility of Floquet Theory for analyzing the performance of orbit maintenance strategies is highlighted. Specifically, transformation of a spacecraft variational state history to modal coordinates is employed to assess the effect of five different orbit maintenance strategies on the state components associated with invariant subspaces of the reference orbit. All of these strategies leverage information available from the linearized variational dynamics near the baseline motion. Two of these strategies, termed Floquet Mode Control strategies, explicitly seek to enact control over the modal coordinates of the spacecraft variational state. The remaining three approaches leverage information available from the STM to define restoring subspaces near the orbit, that result in a decrease in full-state or position magnitude over a specified horizon time. These approaches are termed Principal Stretching Direction Control. All strategies are assessed in the context of an L_2 halo orbit and for a selected mission duration of twenty years, to represent a long-term orbit maintenance scenario.

Dynamical similarities exist between all three effective strategies. Specifically, all successful approaches enact control (explicitly or implicitly) over the unstable component of a spacecraft variational state by constructing orbit maintenance maneuvers that reduce this state component to a near-zero value. These orbit maintenance strategies are also typically associated with an increase in the stable component of the variational state. Of particular importance is the fact that all three of these strategies enact control over the center modes of the orbit as well, particularly the "along family" direction that defines the only subspace of a periodic orbit associated with a variation in the system integral of motion (Jacobi Constant).

Results for the unsuccessful Standard FMC approach indicate that, while control over the unstable component of a spacecraft variational state is necessary for long term stationkeeping, it is not generally sufficient. If an orbit maintenance strategy permits maneuvers that do not maintain the "along family" state component near zero, a drift in phase will occur over time. Maintenance of this "along family" state component can be understood in terms of preventing a variation in energy-like Jacobi Constant from the baseline. Moreover, if a strategy is formulated such that a consistent change in the "along family" component does result, "sliding" of the spacecraft along the family of periodic orbits containing the reference motion is possible. In general, it is therefore recommended that control be enacted over at least both the unstable and "along family" components for long-term

orbit maintenance. Some control may also be required over the quasi-periodic motion associated with the complex center modes of the orbit, at least to prevent excessive growth in this subspace that may invalidate the linearized representation of the dynamics near the baseline orbit.

The cislunar orbit maintenance problem is inherently broad. As such, a variety of avenues could be pursued to extend the present work. Floquet Mode Control strategies would benefit from greater intuition for efficient control over the complex center and "along orbit" subspaces associated with a periodic orbit. An investigation into appropriate selections of the weights necessary for these Floquet Mode Control approaches is warranted. Hybrid strategies, leveraging both the Floquet Mode Control and Stretching Direction Control methodologies are another possible avenue for continued consideration that may yield promising results. The State PSDC methodology, while ineffective in this investigation, allows modification to consider restoring subspaces over longer horizon times, potentially improving results. Finally, all strategies in this investigation should be assessed in a higher-fidelity ephemeris force model and in additional cislunar orbits.

ACKNOWLEDGEMENTS

The authors would like to thank the School of Aeronautics and Astronautics at Purdue University, as well as the Rune and Barbara Eliason Visualization Laboratory, for financial support and facilities. Portions of this work were completed in collaboration with NASA Johnson Space Center and at Purdue University under Grant NASA JSC 80NSSC18M0122. The authors would also like to especially thank Stephen Scheuerle, Brian McCarthy, Emily Zimovan-Spreen, Damennick Henry, and the members of the Purdue Multi-Body Dynamics Research Group for helpful suggestions and discussions.

REFERENCES

[1] "Artemis Plan: NASA's Lunar Exploration Program Overview," Sept. 2020.
[2] D. C. Davis, F. S. Khoury, K. Howell, and D. Sweeney, "Phase Control and Eclipse Avoidance in Near Rectilinear Halo Orbits," *AAS Guidance Navigation and Control Conference*, 2020.
[3] "National Cislunar Science & Technology Strategy," tech. rep., National Science & Technology Council, Nov. 2022.
[4] B. Cheetham, "Cislunar Autonomous Positioning System Technology Operations and Navigation Experiment (CAPSTONE)," *ASCEND 2020*, Virtual Event, American Institute of Aeronautics and Astronautics, Nov. 2020.
[5] D. W. Dunham and C. E. Roberts, "Stationkeeping Techniques for Libration-Point Satellites," *The Journal of the Astronautical Sciences*, Vol. 49, Mar. 2001, pp. 127–144.
[6] D. Folta, T. Pavlak, K. Howell, M. Woodard, and D. Woodfork, "Stationkeeping of Lissajous Trajectories in the Earth-Moon System with Applications to ARTEMIS," *Advances in the Astronautical Sciences*, Vol. 136, Jan. 2010.
[7] D. C. Folta, T. A. Pavlak, A. F. Haapala, K. C. Howell, and M. A. Woodard, "Earth - Moon Libration Point Orbit Stationkeeping: Theory, Modeling, and Operations," *Acta Astronautica*, Vol. 94, Jan. 2014.
[8] D. C. Davis, S. T. Scheuerle, D. A. Williams, F. S. Miguel, E. M. Zimovan-Spreen, and K. C. Howell, "Orbit Maintenance Burn Details for Spacecraft in a Near Rectilinear Halo Orbit," *AAS/AIAA Astrodynamics Specialist Conference*, 2022.
[9] K. Howell and T. Keeter, "Station-Keeping Strategies for Libration Point Orbits: Target Point and Floquet Mode Approaches," *AAS/AIAA Spaceflight Mechanics Meeting*, Feb. 1995.
[10] K. Williams, B. Barden, K. Howell, and R. Wilson, "Genesis Halo Orbit Station Keeping Design," *International Symposium: Space Flight Dynamics*, June 2000.
[11] D. Guzzetti, E. Zimovan, K. Howell, and D. Davis, "Stationkeeping Analysis for Spacecraft in Lunar Near Rectilinear Halo Orbits," *AAS/AIAA Space Flight Mechanics Meeting*, Feb. 2017.
[12] V. Muralidharan and K. C. Howell, "Leveraging stretching directions for stationkeeping in Earth-Moon halo orbits," *Advances in Space Research*, Vol. 69, Jan. 2022, pp. 620–646.
[13] D. A. P. Williams, K. C. Howell, and D. C. Davis, "A Comparison of Station-Keeping Strategies for Halo Orbits," *AAS/AIAA Astrodynamics Specialist Conference*, Aug. 2023.
[14] C. Simó, G. Gómez, J. Llibre, and R. Martinez, "Stationkeeping of a quasiperiodic halo orbit using invariant manifolds," *Proceedings of the Second International Symposium on Spacecraft Flight Dynamics*, 1986.

[15] C. Simó, G. Gómez, J. Llibre, R. Martínez, and J. Rodríguez, "On the Optimal Station Keeping Control of Halo Orbits," *Acta Astronautica*, Vol. 15, June 1987, pp. 391–397.

[16] G. Gómez, K. Howell, J. Masdemont, and C. Simó, "Station-Keeping Strategies For Translunar Libration Point Orbits," *Advances in the Astronautical Sciences*, Vol. 99, Jan. 1998.

[17] A. Farrés, C. Gao, J. J. Masdemont, G. Gómez, D. C. Folta, and C. Webster, "Geometrical Analysis of Station-Keeping Strategies About Libration Point Orbits," *Journal of Guidance, Control, and Dynamics*, Vol. 45, June 2022, pp. 1108–1125.

[18] A. Cox, *A Dynamical Systems Perspective for Preliminary Low-Thrust Trajectory Design in Multi-Body Regimes*. PhD Dissertation, Purdue University, West Lafayette, IN, May 2020.

[19] D. A. P. Williams, *Dynamics of Long-Term Orbit Maintenance Strategies in the Circular Restricted Three Body Problem*. Master's thesis, Purdue University, 2024.

[20] Y. Tsuda and D. J. Scheeres, "Numerical Method of Symplectic State Transition Matrix and Application to Fully Perturbed Earth Orbit," *Transactions of the Japan Society for Aeronautical and Space Sciences*, Vol. 53, No. 180, 2010, pp. 105–113.

[21] J. D. Hadjedemetriou, "Periodic orbits in gravitational systems," *Chaotic Worlds: From Order to Disorder in Gravitational N-Body Dynamical Systems* (B. A. Steves, A. J. Maciejewski, and M. Hendry, eds.), Dordrecht, Springer Netherlands, 2006, pp. 43–79.

[22] E. Zimovan, K. Howell, and D. Davis, "Near rectilinear halo orbits and nearby higher-period dynamical structures: orbital stability and resonance properties," *Celestial Mechanics and Dynamical Astronomy*, Vol. 132, June 2020.